

Supplementary Information

Controlling Nanocluster Growth through Nanoconfinement: The Effect of the Number and Nature of Metal-Organic Framework Functionalities

By James King, Zhipeng Lin, Federica Zanca, Hui Luo, Linda Zhang, Patrick Cullen, Mohsen Danaie, Michael Hirscher, Simone Meloni, Alin M. Elena, and Petra Á. Szilágyi*

*p.a.szilagyi@kjemi.uio.no

Table of contents

1. Additional experimental details.....	1
2. Additional experimental data.....	2
2.1. PXRD	2
2.2. STEM and EDX spectroscopy	3
2.3. XPS	4
2.4. TDS	5
2.5. BET specific surface areas	6
3. Additional computational details.....	6
4. References.....	12

1. Additional experimental details

Table S1 Quantities and reagents for the MOF syntheses.

MOF	Ligand	Ligand/ mmol	ZrCl ₄ /mmol	Volume HCl /ml	Volume DMF /ml
(NH ₂) ₂ -UiO-66	2,5-diamino- benzenedicarboxylic acid	0.54	0.75	1	15
CH ₃ -UiO-66	2-methyl- benzenedicarboxylic acid	0.54	0.75	1	15
(CH ₃) ₂ -UiO-66	2,5-dimethyl- benzenedicarboxylic acid	0.54	0.75	1	15

2. Additional experimental data

2.1 PXRD

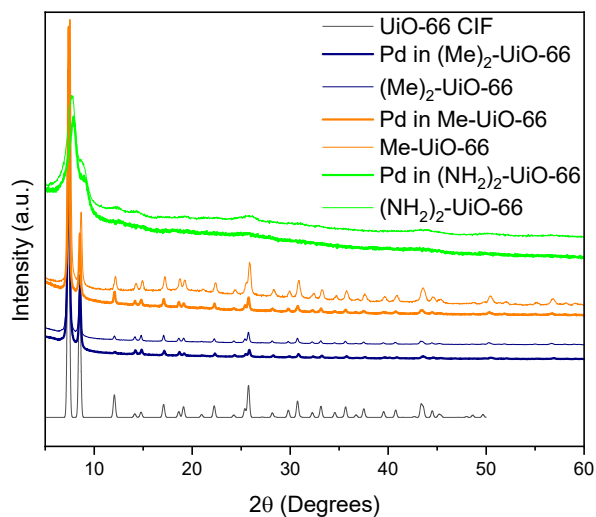


Figure S1 XRD patterns for the empty and Pd-laden MOFs, including the pattern for pristine UiO-66 generated from its CIF file¹.

2.2 STEM micrographs

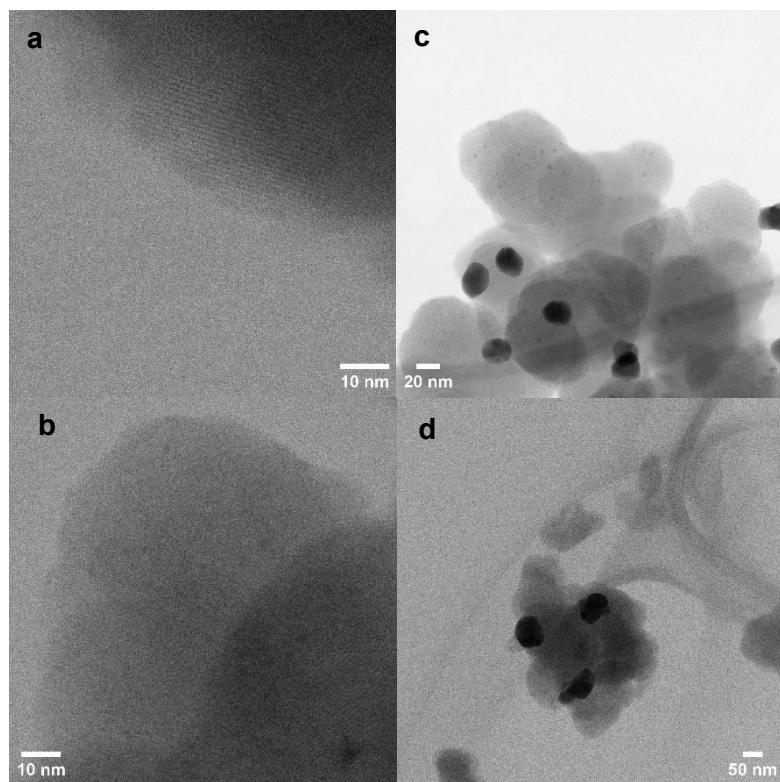


Figure S2 Complementary bright-field TEM micrographs of those in figure 1 of a) Pd in $(NH_2)_2$ -UiO-66, b) and c) Pd in CH_3 -UiO-66 and d) Pd in $(CH_3)_2$ -UiO-66, demonstrating the extent of embedment of Pd (dark spots) in the frameworks.

2.2 EDX Spectroscopy

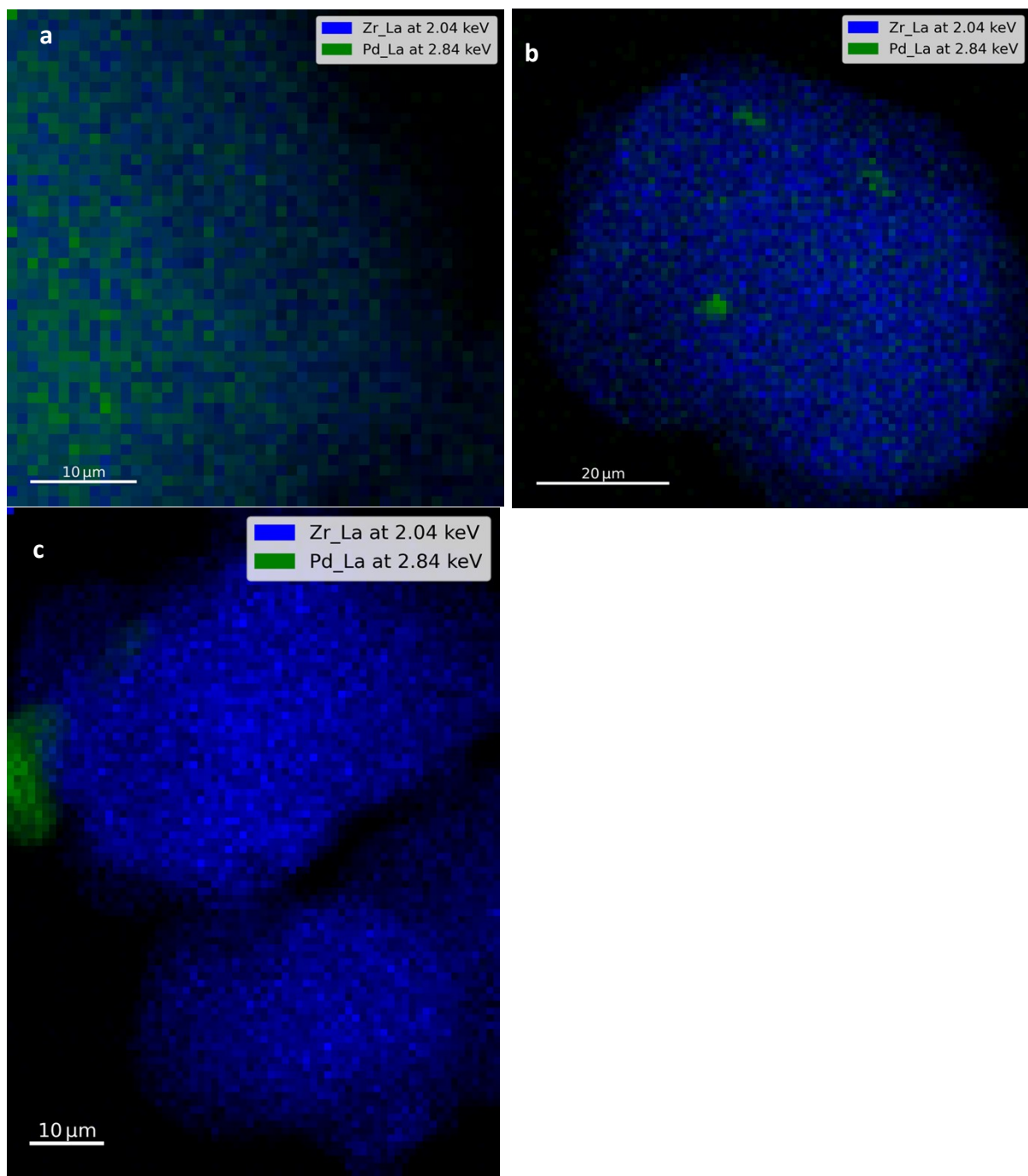


Figure S3 Reconstructed EDX maps for a) Pd in $(\text{NH}_2)_2\text{-UiO-66}$, b) Pd in $\text{CH}_3\text{-UiO-66}$ and c) Pd in $(\text{CH}_3)_2\text{-UiO-66}$, overlaying signals from Zr (blue) with those from Pd (green).

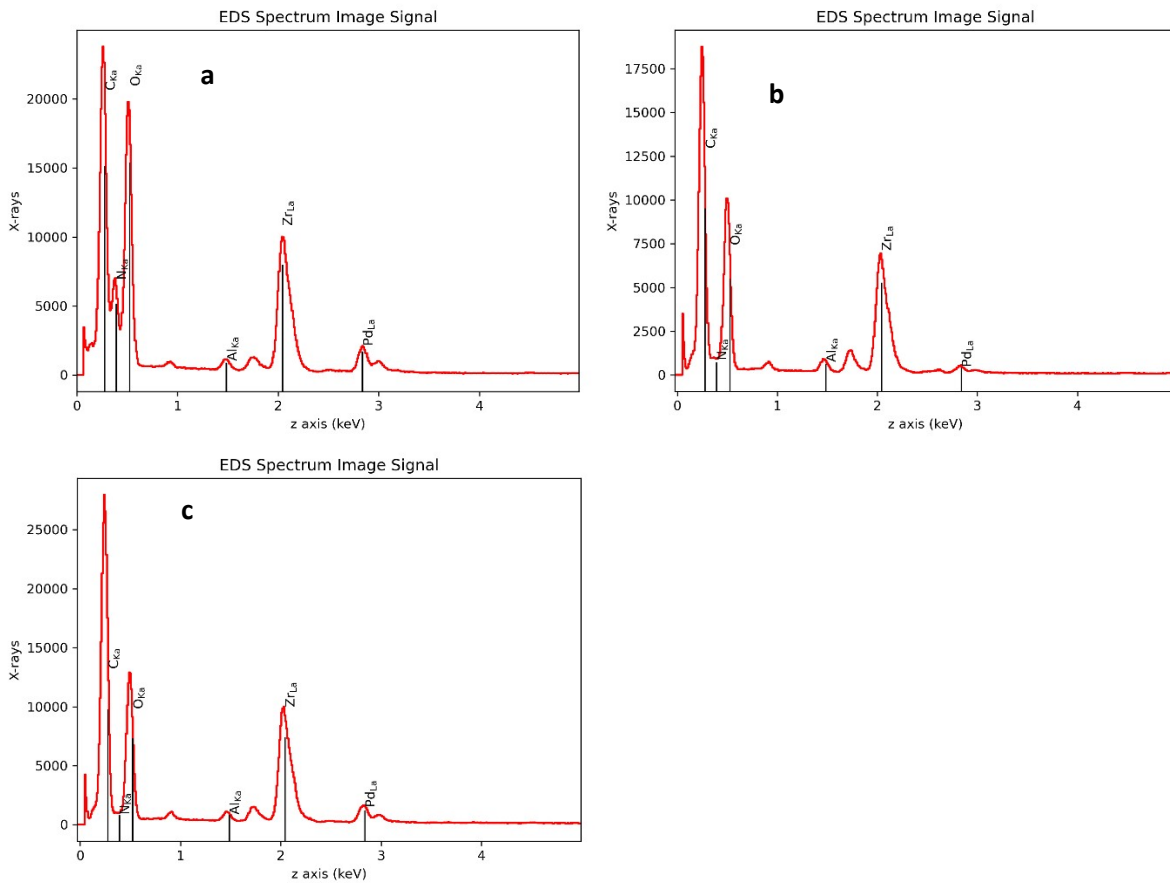


Figure S4 EDX spectra of a) Pd in $(\text{NH}_2)_2\text{-UiO-66}$, b) $\text{CH}_3\text{-UiO-66}$ and c) $(\text{CH}_3)_2\text{-UiO-66}$.

2.3 XPS

Table S2 XPS peak positions of data presented in figure 2 for the Pd-laden MOF samples.

XPS peak assignment	XPS peak position, [eV]		
	Pd in $(\text{NH}_2)_2\text{-UiO-66}$	Pd in $\text{CH}_3\text{-UiO-66}$	Pd in $(\text{CH}_3)_2\text{-UiO-66}$
Zr $3p_{3/2}$	333.7	333.8	333.5
Zr $3p_{1/2}$	347.3	347.4	347.1
Pd $3d_{5/2}$	335.9	335.8	335.8
Pd $3d_{3/2}$	341.2	341.1	341.1
Pd oxidised* $3d_{5/2}$	337.7	337.7	336.8
Pd oxidised* $3d_{3/2}$	343.2	343.0	342.1
N 1s	399.7	n/a	n/a
N 1s (2)	401.2	n/a	n/a
C 1s C-C	n/a	284.8	284.8
C 1s C-O-C	n/a	286.3	286.4
C 1s O-C=O	n/a	288.6	288.7

* This surface-oxidised PdO signal is most likely due to the samples' exposure to some air despite our best efforts.

Table S3 XPS peak positions of data for the empty MOF samples for functional group element binding energy comparisons upon introduction of Pd.

XPS peak assignment	XPS peak position, [eV]		
	(NH ₂) ₂ -UiO-66	CH ₃ -UiO-66	(CH ₃) ₂ -UiO-66
N 1s	399.1	n/a	n/a
N 1s	401.1	n/a	n/a
C 1s C-C	n/a	284.8	284.8
C 1s C-O-C	n/a	286.3	286.4
C 1s O-C=O	n/a	288.9	288.7

Table S4 Pd:Zr elemental ratio determined from XPS spectra for the various MOF host matrices.

MOF matrix	NH ₂ -UiO-66	(NH ₂) ₂ -UiO-66	CH ₃ -UiO-66	(CH ₃) ₂ -UiO-66
Pd:Zr ratio	0.7	0.8	0.9	0.6

2.4 TDS

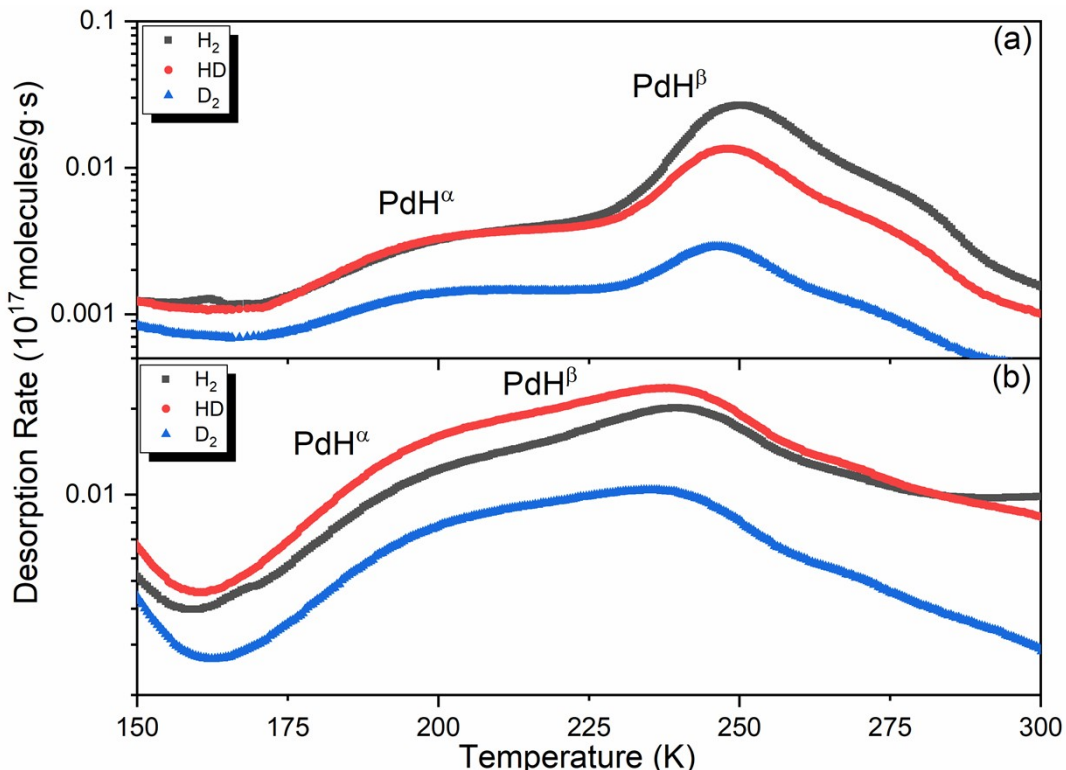


Figure S5 TDS spectra of the exposure of 50 mbar 1:1 D₂/H₂ mixture on a) Pd in (NH₂)₂-UiO-66 and b) Pd in Br-UiO-66 at room temperature after cooling to 20 K, with a heating rate of 0.1 K s⁻¹.

2.5 BET

Table S5 BET specific surface areas.

MOF	BET m ² g ⁻¹
NH ₂ -UiO-66	1122
Pd in NH ₂ -UiO-66	790
(NH ₂) ₂ -UiO-66	62
Pd in (NH ₂) ₂ -UiO-66	76
CH ₃ -UiO-66	873
Pd / CH ₃ -UiO-66	751
(CH ₃) ₂ -UiO-66	661
Pd / (CH ₃) ₂ -UiO-66	708

3. Additional computational details

Table S6. Bonding energies (eV) of Pd(NO₃)₂ and Pd⁰.

	Pd(NO ₃) ₂ bonding energy (eV)	MOF+Pd(NO ₃) ₂ total energy (eV)	Pd-functional group distance	Pd-C _{benzene}	Pd-N (NO ₃)
CH ₃ -UiO-66 1	-0.738807141	-38801.28419	4.6	3.5	2.47
CH ₃ -UiO-66 2	-5.049108719	-38784.76584	6.3	3.3	3.1
(CH ₃) ₂ -UiO-66 1	-0.849644784	-40012.48119	3.8	3.4	2.47
(CH ₃) ₂ -UiO-66 2	-2.016929014	-39992.84096	4	2.2	2.8
NH ₂ -UiO-66 1	0.421630426	-39360.16459	4.5	3.5	2.47
NH ₂ -UiO-66 2	-2.634719949	-39361.59894	3.3	2.14	2.52
(NH ₂) ₂ -UiO-66 1	-0.796587573	-41131.03553	3.7	3.1	2.48
(NH ₂) ₂ -UiO-66 2	-5.767623769	-41131.85656	2.6	2.12	2.6

Table S7. Calculated values for adsorption energy of Pd nanocluster (17 atoms) in eV. The adsorption energy is calculated as $E_{\text{ads}} = E_{\text{tot}} - E_{\text{Pd}} - E_{\text{MOF}}$. Calculated distances between the functional group and the Pd cluster.

	Pd ₁₇ bonding energy (eV)	Pd-N distance (Å)	Pd-C _{benzene} distance (Å)	Pd-C _{functional} distance (Å)	Functional group – benzene bond length (Å)
CH ₃ -UiO-66-Pd	-5.53		2.18	3.8	1.5
(CH ₃) ₂ -UiO-66-Pd	-7.59		2.18	2.5-3	1.5
NH ₂ -UiO-66-Pd	-13.23	2.26	2.22		1.38
(NH ₂) ₂ -UiO-66-Pd	-16.59	2.14	2.18		1.36

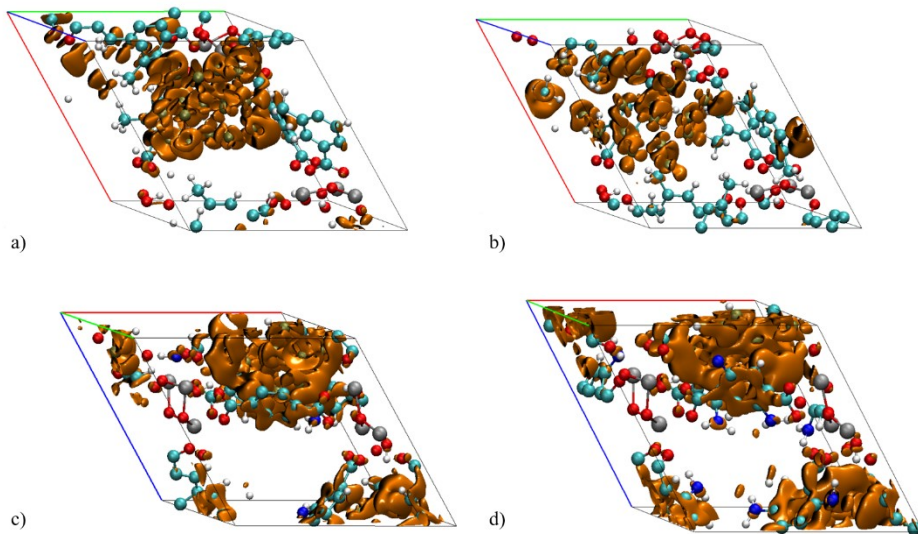


Figure S6 Charge transfer (in orange) for a) $\text{CH}_3\text{-UiO-66-Pd}$ b) $(\text{CH}_3)_2\text{-UiO-66-Pd}$ c) $\text{NH}_2\text{-UiO-66-Pd}$ d) $(\text{NH}_2)_2\text{-UiO-66-Pd}$. C: cyan, H: white, N: blue, O: red, Pd: ochre, Zr: grey

Table S8 Cumulative charge values on the central atoms of the linker functional groups (N or C, N for NH_2 and C for CH_3) in the fully loaded MOFs, empty MOFs, as well as on the Pd_{17} cluster in the respective MOF.

	Functional group charge in loaded MOF	Functional group charge in empty MOF	C in loaded MOF	C in empty MOF	Pd charge
$\text{CH}_3\text{-UiO-66}$	-0.037631	2.60E-05	31.325494	31.99	0.22
$(\text{CH}_3)_2\text{-UiO-66}$	-0.342618	-0.118585	31.718308	32.020354	0.6
$\text{NH}_2\text{-UiO-66}$	-11.1	-10.41			0.74
$(\text{NH}_2)_2\text{-UiO-66}$	-21.45	-20.75			0.59

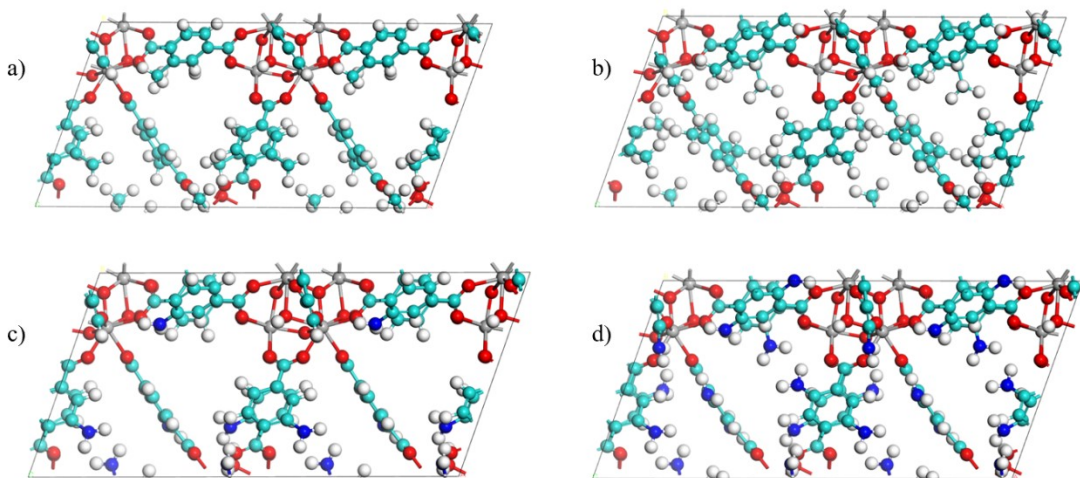


Figure S7. Optimised MOF geometries in a $2 \times 1 \times 1$ supercell. The structure is optimised in a single cell, that is here repeated in a direction for better comparison with Figure S8. a) $\text{CH}_3\text{-UiO-66}$ b) $(\text{CH}_3)_2\text{-UiO-66}$ c) $\text{NH}_2\text{-UiO-66}$ d) $(\text{NH}_2)_2\text{-UiO-66}$. C: cyan, H: white, N: blue, O: red, Zr: grey.

Optimised cell parameters for the MOFs:

$\text{CH}_3\text{-UiO-66}$: A=14.77 Å, B=14.77 Å, C= 14.77 Å, $\alpha=59.96^\circ$, $\beta=59.93^\circ$, $\gamma=59.95^\circ$, V= 2277.06 Å³
 $(\text{CH}_3)_2\text{-UiO-66}$: A=14.77 Å, B=14.77 Å, C= 14.77 Å, $\alpha=59.99^\circ$, $\beta=59.98^\circ$, $\gamma=59.98^\circ$, V= 2279.76 Å³
 $\text{NH}_2\text{-UiO-66}$: A=14.78 Å, B=14.77 Å, C= 14.75 Å, $\alpha=59.94^\circ$, $\beta=59.9^\circ$, $\gamma=59.9^\circ$, V = 2273.71 Å³
 $(\text{NH}_2)_2\text{-UiO-66}$: A=14.75 Å, B=14.77 Å, C= 14.75 Å, $\alpha=60.08^\circ$, $\beta=60.01^\circ$, $\gamma=59.95^\circ$, V= 2274.85 Å³

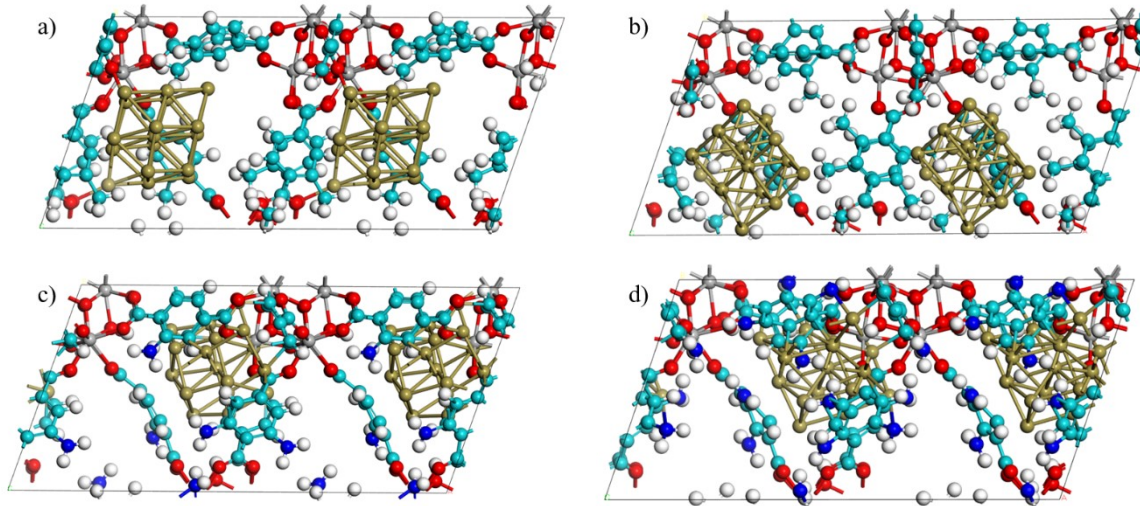


Figure S8. Optimised MOF-Pd geometries in a 2x1x1 supercell. The structure is optimised in a single cell, that is here repeated in a direction to better illustrate how the Pd is inserted. a) Pd in $\text{CH}_3\text{-UiO-66}$ b) Pd in $(\text{CH}_3)_2\text{-UiO-66}$ c) Pd in $\text{NH}_2\text{-UiO-66}$ d) Pd in $(\text{NH}_2)_2\text{-UiO-66}$. C: cyan, H: white, N: blue, O: red, Pd: ochre, Zr: grey.

Optimised cell parameters for MOF-Pd:

$\text{CH}_3\text{-UiO-66-Pd}$: A=14.78 Å, B=14.64 Å, C= 14.77 Å, $\alpha=59.36^\circ$, $\beta=59.10^\circ$, $\gamma=59.9^\circ$, V = 2232.88 Å³
 $(\text{CH}_3)_2\text{-UiO-66-Pd}$ A=14.72 Å, B=14.69 Å, C= 14.71 Å, $\alpha=60.2^\circ$, $\beta=59.79^\circ$, $\gamma=60^\circ$, V = 2255.36 Å³
 $\text{NH}_2\text{-UiO-66-Pd}$ A=14.74 Å, B=14.64 Å, C= 14.52 Å, $\alpha=60.22^\circ$, $\beta=59.99^\circ$, $\gamma=60.2^\circ$, V = 2224.29 Å³
 $(\text{NH}_2)_2\text{-UiO-66-Pd}$ A=14.31 Å, B=14.65 Å, C= 14.77 Å, $\alpha=60.43^\circ$, $\beta=60.36^\circ$, $\gamma=60.94^\circ$, V = 2219.92 Å³

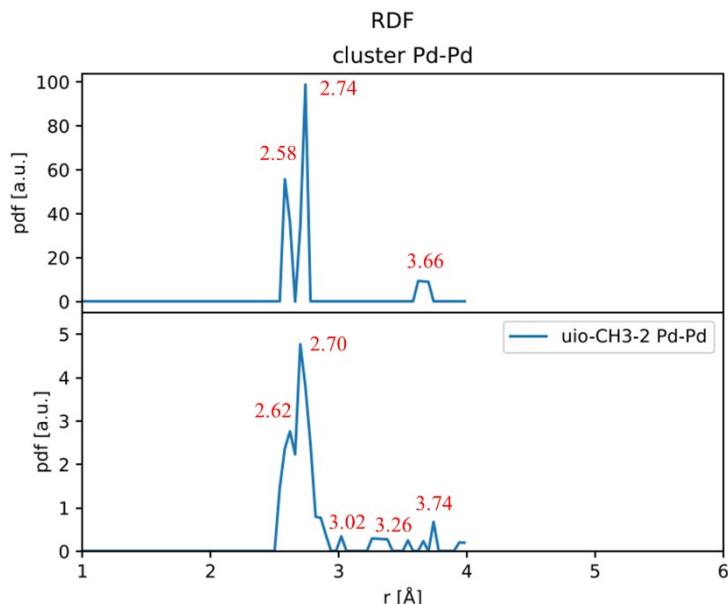


Figure S9 Pd-Pd distances in cluster only for Pd in $(\text{CH}_3)_2\text{-UiO-66}$.

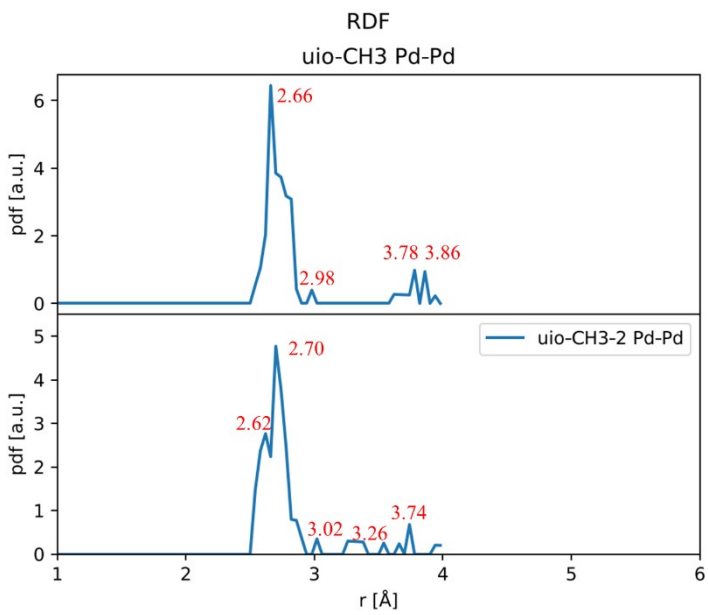


Figure S10 Pd-Pd distances in only for Pd in CH₃-UiO-66, and in (CH₃)₂-UiO-66. Cluster appears to be more distorted in (CH₃)₂-UiO-66 than in CH₃-UiO-66.

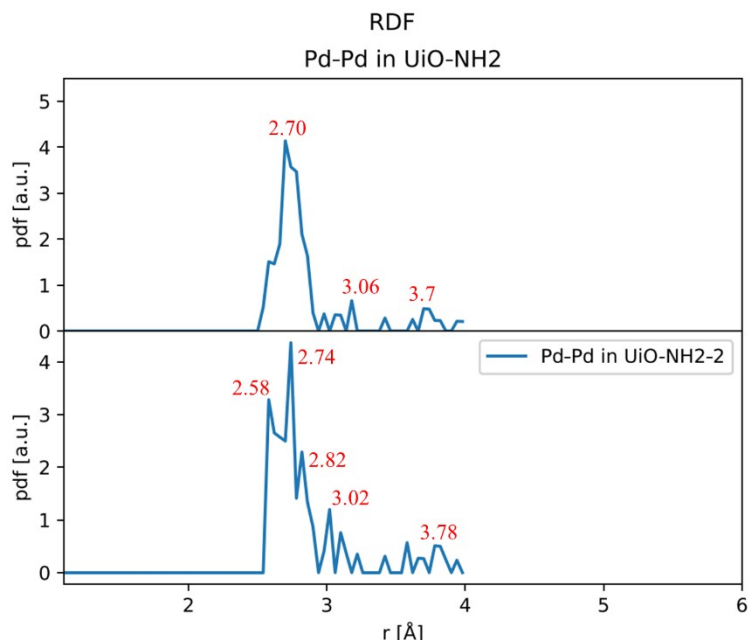


Figure S11 Pd-Pd distances in only for Pd in NH₂-UiO-66, and in (NH₂)₂-UiO-66.

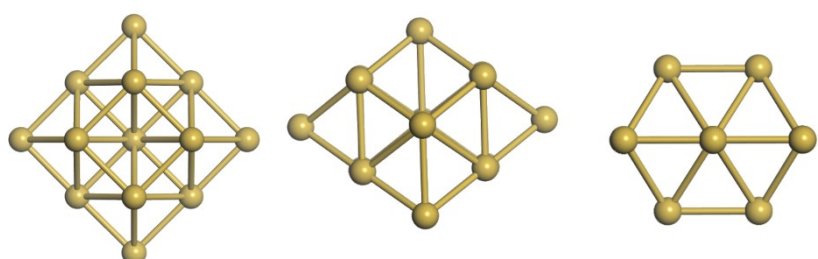


Figure S12 Ideal Pd₁₇ cluster.

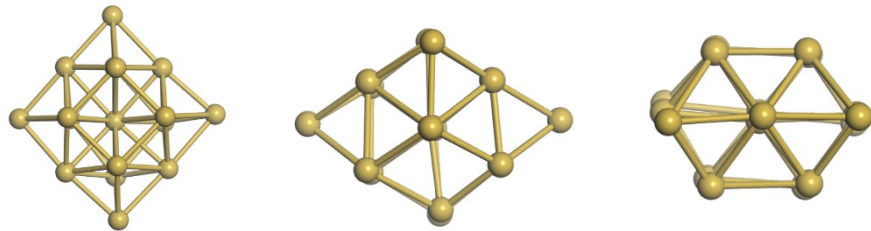


Figure S13 Pd_{17} cluster in $\text{CH}_3\text{-UiO-66}$.

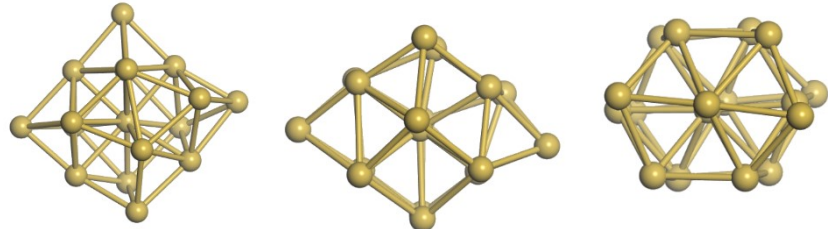


Figure S14 Pd_{17} cluster in $(\text{CH}_3)_2\text{-UiO-66}$.

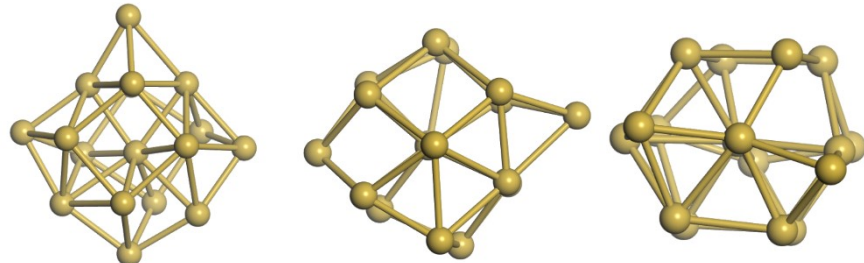


Figure S15 Pd_{17} cluster in $\text{NH}_2\text{-UiO-66}$.

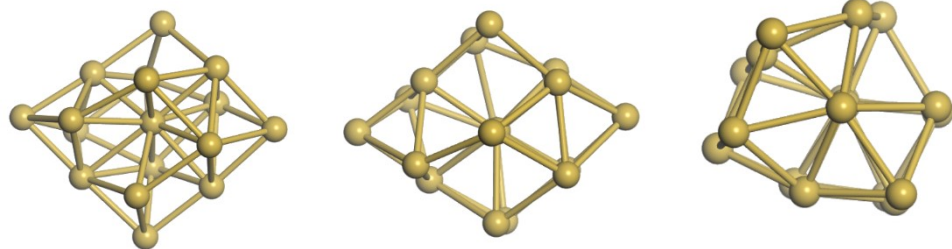


Figure S16 Pd_{17} cluster in $(\text{NH}_2)_2\text{-UiO-66}$

Table S9. Distances between Pd^0 and Pd^{2+} and C or N in Å.

	Pd ⁰ -C	Pd ²⁺ -C	Binding site Pd ⁰	Binding site Pd ²⁺
CH ₃ -UiO-66	2.22	3.26	C _{benzene}	O
(CH ₃) ₂ -UiO-66	2.25	2.25	C _{benzene}	C _{benzene}
	Pd ⁰ -N	Pd ²⁺ -N		
NH ₂ -UiO-66	2.5	3.3	C _{benzene} (Pd-C distance=2.14)	C _{benzene} (Pd-C distance=2.14)
(NH ₂) ₂ -UiO-66	2.14	2.6	NH ₂	C _{benzene} (Pd-C distance=2.12)

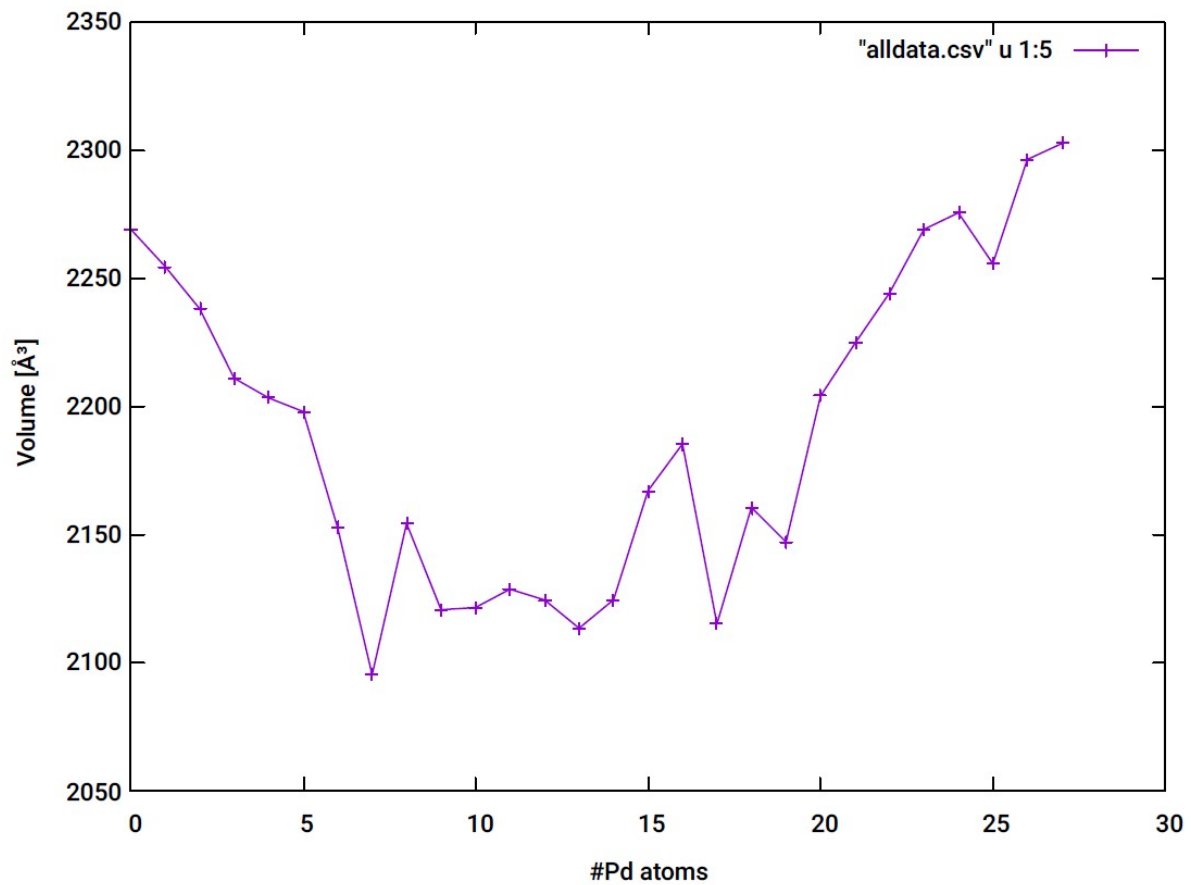


Figure S17 MOF equilibrium volume as predicted from molecular simulations. We notice a minimum volume in the region of NC of size 6-17 atoms.

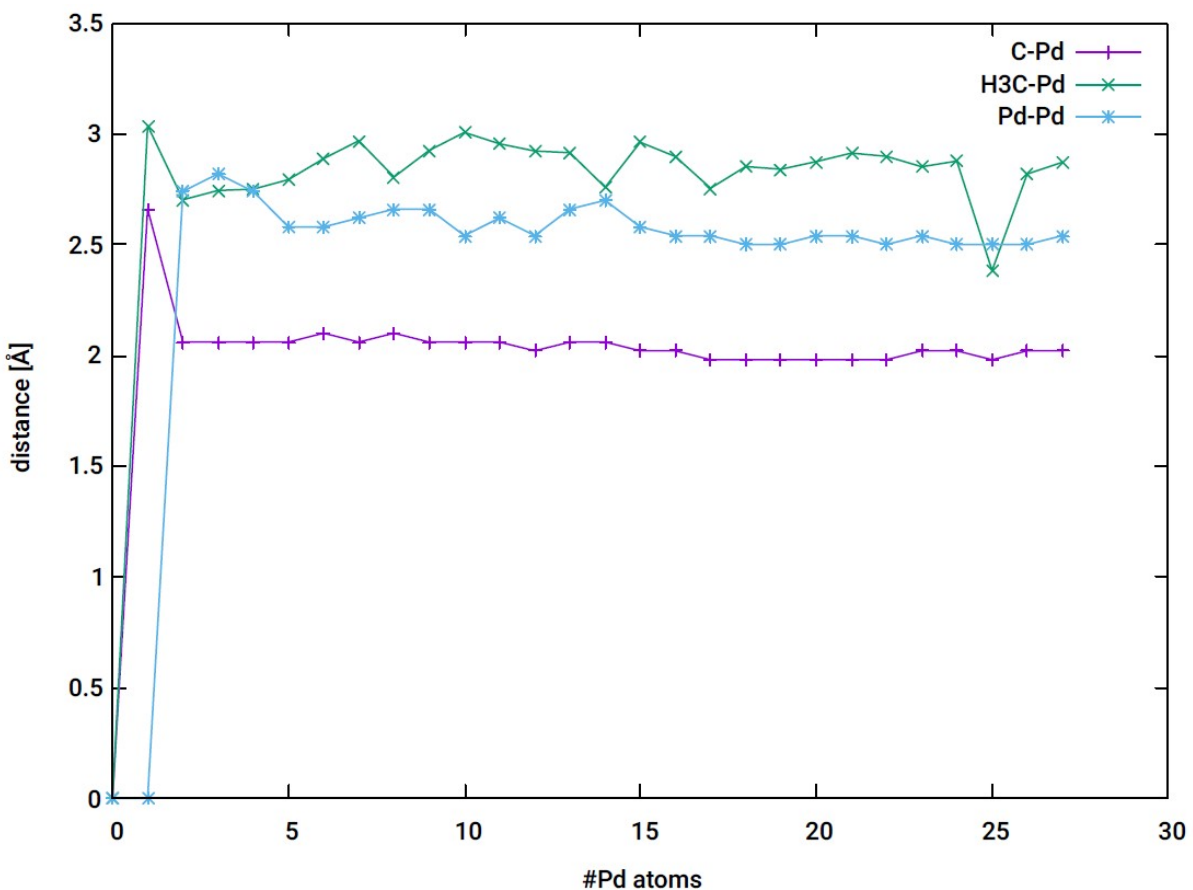


Figure S18 Minimum distances between various species, Pd-C and C from methyl group and Pd and Pd-Pd surprisingly after adding as few as 3 Pd atoms in the molecular simulations predict practically constant distances for all three sets.

4. References

- (1) Øien, S.; Wragg, D.; Reinsch, H.; Svelle, S.; Bordiga, S.; Lamberti, C.; Lillerud, K. P. Detailed Structure Analysis of Atomic Positions and Defects in Zirconium Metal-Organic Frameworks. *Cryst. Growth Des.* **2014**, *14* (11), 5370–5372.